



Experimental Study on Puncture Resistance of 2D and 3D Glass Fabrics Reinforced with Shear Thickening Fluid

M. Jeddi^{1,2}, M. Yazdani^{1,2*}, H. Hasan-nezhad^{1,2}

¹Department of Mechanical Engineering, Sahand University of Technology, Tabriz, Iran

²Dynamic Behavior of Materials Research Laboratory, Sahand University of Technology, Tabriz, Iran

ABSTRACT: In this study, the quasi-static puncture resistance of neat and shear thickening fluid impregnated Kevlar, 2D, and 3D-glass fabrics were investigated using a universal testing machine. For the synthesis of the shear thickening fluid, silica nanoparticles were dispersed in polyethylene glycol in the mass fraction of 20, 25, 30, and 35 wt%. The influence of the shear thickening fluid concentration on the puncture resistance of the impregnated 3D-glass fabrics was examined and compared with the neat samples. The results revealed the puncture resistance of the impregnated 3D-glass fabrics increased with raising the concentration from 20 to 30 wt% (637 to 688 N). However, the performance of the 35 wt% impregnated sample was reduced (657 N). The 30 wt% impregnated 3D-glass fabric showed the most puncture resistance, such that its peak force (688 N) was 17% higher than the neat case (590 N). The results were compared with those of Kevlar and four-ply 2D-glass fabrics, and it was observed that the 30 wt% effect on the 3D fabrics was more evident than them. Unlike the 2D-glass fabrics, the bending angle (θ) for the 3D-glass fabrics decreased by 10° and as a result, their flexibility lessened. The thickness of the impregnated 2D-glass fabric increased more than the 3D fabrics (27% vs. 4%).

Review History:

Received: Apr. 24, 2021

Revised: Aug. 16, 2021

Accepted: Oct. 09, 2021

Available Online: Oct. 11, 2021

Keywords:

Shear thickening fluid

Quasi-static loading

Puncture test

Glass fiber reinforced polymer

1- Introduction

The use of novel and lightweight materials as a structural reinforcement with low cost and high-performance capabilities plays a considerable role in improving protective cloths and flexible composite structures. This is why researchers have studied the stab or puncture resistance of composites to enhance the protective efficiency of clothing [1-3]. Researchers are constantly trying to enhance the performance of soft body armors. Most previous studies about quasi-static puncture resistance have focused on high-strength and high-modulus fibers such as carbon fibers, aramid fibers (Kevlar), and Ultra-High Molecular Weight Polyethylene (UHMWPE) fibers, etc [4]. The main factor limiting the usage of this type of material is their high price, such that in some cases the protection level is not that high and we could use alternative materials instead of these expensive fibers. Considerable attention has been given to the use of textiles like Glass Fiber-Reinforced Polymer (GFRP) composite in both industry and academia due to their high specific strength and stiffness, also the considerable effect of their structure on the protective performance [2, 5]. Two-Dimensional (2D) fabrics have been widely applied in composite structures over decades. Recently it was found that one of the suitable materials to improve the resistance of composites is the Three-Dimensional (3D) fabrics, which can overcome many delamination problems by

filling the spaces among the fibers with various mediums [6]. Therefore, 3D woven composites have received increasing attention from various engineering sectors because of their numerous structural advantages [7, 8]. Spacer fabrics are 3D textiles typically consisting of two discrete fabrics connected by vertical pile yarns, which have been introduced in recent papers as basic materials for composites [9, 10]. The fibers of the aramid class, e.g., Kevlar®, Twaron®, etc. have been investigated broadly as basic materials for soft body armors and it has become clear that their mechanical properties could be improved by impregnating them with Shear Thickening Fluids (STFs) [11, 12].

The STF is a non-Newtonian fluid, which shows a reversible shear-thickening behavior (rapid rise in viscosity) with increasing the applied shear rate and occurs in most colloidal suspensions [2, 13, 14]. Employing the STF to enhance the ballistic or puncture resistance of materials, has interested attention and demonstrates a better protection performance as compared with neat (non-impregnated) fabrics [15, 16]. The most investigation related to the STFs has been limited to the impregnated Kevlar and p-aramid [12, 15-21]. In the case of the STF, the suspension of silica nanoparticles in the Polyethylene Glycol (PEG) has been broadly investigated and mostly reported in the papers [11]. The possible reasons for the reversible shear-thickening behavior have been suggested as the order-disorder transition, the hydrocluster, and contact rheology model mechanism

*Corresponding author's email: m.yazdani@sut.ac.ir



Table 1. Specification of the fabrics used in this study

Fabric	Weave Pattern	Areal Density (g/m ²)
3D E-Glass	3D (PARAGLASS-Type 5)	840
2D E-Glass	Plain weave	200
Kevlar	Twill weave	400

Table 2. The STFs investigated in the present work

STF Type	Dispersed Particles in PEG	Weight Percent (wt%)
STF20	Silica nano-particles	20
STF25	Silica nano-particles	25
STF30	Silica nano-particles	30
STF35	Silica nano-particles	35

[22]. The order-disorder mechanism explains that because of particle interactions at the time of low shear-rate, an arranged laminar flow disrupts into a disordered viscous flow at high shear-rates [23]. The hydrocluster mechanism shows that the formation of clusters of the particles is related to hydrodynamic lubrication forces, which leads to the shear-thickening behavior and it's reversible due to the breakups of the clusters [24]. A new mechanism, namely the contact rheology model is proposed in recent papers [25, 26]. It is declared that the hydro-clustering prevails suspensions at low shear-rates because of contactless rheology; since particle pressure is not enough to overcome the repulsion among the particles. The contact forces become stronger at the point of the shear-thickening where the colloidal particles contact each other. To the further increase in the shear-rate, the contact forces generate force networks that dominate the thickening where the hydrodynamic interactions are claimed to be insufficient. It has become clear that the rheological properties of the STFs depend on many factors like the concentration of suspended particles and additive materials [27].

The development of low cost, lightweight, and wearable protection clothing is the main objective of body armor researches. As mentioned the most papers related to the STFs have been limited to Kevlar and p-aramid fabrics. Considering the high price of Kevlar fabrics and the ever-increasing use of glass fibers as reinforcement in various composites; in this research, the quasi-static puncture resistance of the neat (non-impregnated) and Shear Thickening Fluid (STF) impregnated Kevlar, 2D, and 3D-glass fabrics were investigated. An innovative aspect of this study lies in employing the 3D-glass fabrics impregnated with the STF in various concentrations and studying the effect of the STF impregnation on their puncture resistance, flexibility, and thickness, as well as

comparing their performance with 2D and Kevlar fabrics. In this research, the STF mixture was prepared by dispersing silica nanoparticles (12 nm) in the Polyethylene Glycol (PEG) with a molecular weight of 400 g/mol using the combination of mechanical mixing and the sonication method. The influence of the STF concentration on the performance of the samples against puncture loading was empirically investigated. The puncture resistance of 20, 25, 30, and 35 wt% STF impregnated samples were studied, and the best STF concentration was obtained. The best performance of the 3D-glass fabric was compared with Kevlar and 2D-glass fabrics.

2- Experimental

2- 1- Materials

The materials employed in this study include 2D E-glass, Kevlar, and 3D E-glass fabrics with a thickness of 5 mm made by the Parabeam industries (Netherlands), the details of which are given in Table 1.

The STF was made with fumed silica, purchased from the Evonik Degussa Co (Aerosil 200), Germany, and according to the supplier is hydrophilic and has a particle size of 12 nanometers. The carrier fluid in this research as a liquid polymer is Polyethylene Glycol (PEG) with an average molecular weight of 400 (g/mol) from Merck (Germany). Ethanol (Ethyl alcohol 96 medical-grade) from Kimia Alcohol Zanjan Co (Iran) was used for diluting the STF.

2- 2- Synthesis of STF

In this work, various STFs with four types of silica concentration were prepared, the details of which are summarized in Table 2.

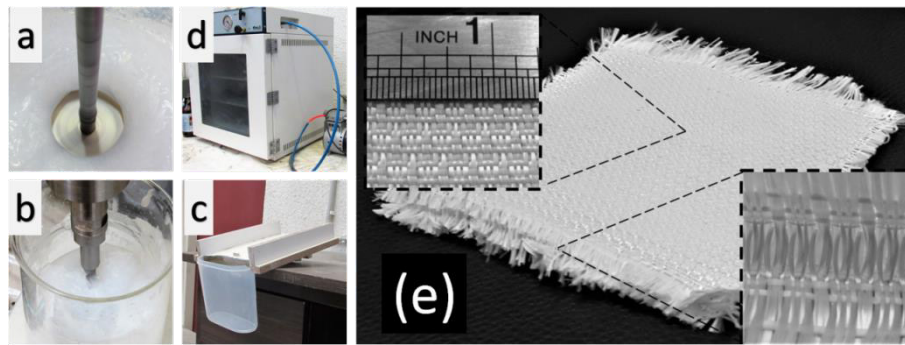


Fig. 1. Steps of STF preparation and fabric impregnation: (a) mechanical blending to homogenization, (b) ultra-sonication, (c) the container with an inclined plane, (d) the oven to evaporate the ethanol, (e) 3D E-glass fabric PARAGLASS (type 5).

For the synthesis of the STFs, the combination of mechanical mixing and sonication method was used. Employing the mechanical mixing method, the STF suspensions were prepared by dispersion of 20 wt%, 25 wt%, 30 wt%, and 35 wt% silica nanoparticles into the PEG. First, a small amount of the silica nanoparticles was added to the PEG and then blended by a mixer (MTOPS-HD1200D, Korea) for 15 min at 500 rpm, and it has repeated at 1000 and 1500 rpm for 15 min for each step (see Fig. 1a). For homogeneity of the mixture according to previous studies, mechanical and ultrasonic mixing methods have been used [28]. Therefore, among the blending steps, a little deal of the silica nanoparticles was added to the suspension up to the required concentration, such that the homogeneous suspension was gained. Ethanol can be easily evaporated, so it was used as a solvent in the fabrication of the STF impregnated samples (see Fig. 1e) in the mass ratio of 4; STF: ethanol = 1:4, in order to facilitate the impregnation process. In the next step, the blended suspension was sonicated by the ultrasonic horn (Hielscher-UP400S, Germany) in 0.5 cycle and 30% amplitude for 15 m (see Fig. 1b). As previous investigations have shown, the ultrasound sonication method is an effective way in the preparation of the STF [25].

2- 3- Fabrication of STF/fabric composite

The fabrics were cut in square format (127×127 mm). After the cutting step, ten layers of fabrics were placed in one package to carefully weigh them by a digital scale. Therefore, the average neat weight of each layer was determined. Each package of neat fabrics (10 samples) was impregnated with the ethanol/STF suspension by the dip-coating procedure in a container with an inclined plane (see Fig. 1c). After the soaking step, each dipped layer was placed on the inclined plane and was padded with the ethanol/STF by a steel padding roller of 0.9 kg. The padding roller only by its weight force slipped down and by exerting pressure on the impregnated samples, the excess STF of the samples was

removed. Afterward, the impregnated layers were placed in an oven at 70°C for six hours [15] to evaporate and remove the ethanol (Fig. 1d). In the end, the samples were weighed again to obtain the average impregnated weight of the layers.

2- 4- Rheological properties

The STFs were prepared by dispersion of the fumed silica nanoparticles in the PEG in four different concentrations. It is worth mentioning the main objective of this work is to carefully study the puncture resistance of the STF impregnated 2D and 3D-glass fabrics. However, since not all silica/PEG suspensions exhibit shear-thickening behavior, the rheological tests were carried out on all the STFs to observe their behavior. A dynamic rheometer (MCR301: Anton Paar, Austria) was used to measure the rheological characteristics of the 20, 25, 30, and 35 wt% STF using the parallel plate geometry. The diameter of both upper and lower plates was 25 mm and the gap between the two parallel plates was 1 mm. The rheological measurements were carried out at room temperature. Therefore, shear-rate sweep test was made in the range of 0.147 to 215 s⁻¹. The corresponding logarithmic diagram (viscosity versus shear-rate) is shown in Fig. 2.

As illustrated in the figure, both behaviors of shear-thinning and shear-thickening can be seen. At high shear-rates in the shear-thickening region, the high-concentrated STF exhibits a considerable increase in viscosity, and increasing the concentration of the STF leads to a decrease in the critical shear-rate.

2- 5- Field Emission Scanning Electron Microscopy (FE-SEM) images

FE-SEM analysis is a suitable method to investigate the superficial morphology of the coated samples. Therefore, the FE-SEM analysis was employed just to examine the coating quality of the STF on the impregnated fabric. Fig. 3 shows the FE-SEM results of the STF impregnated 3D-glass fabrics with 30 wt% silica nanoparticles. The FE-SEM analysis

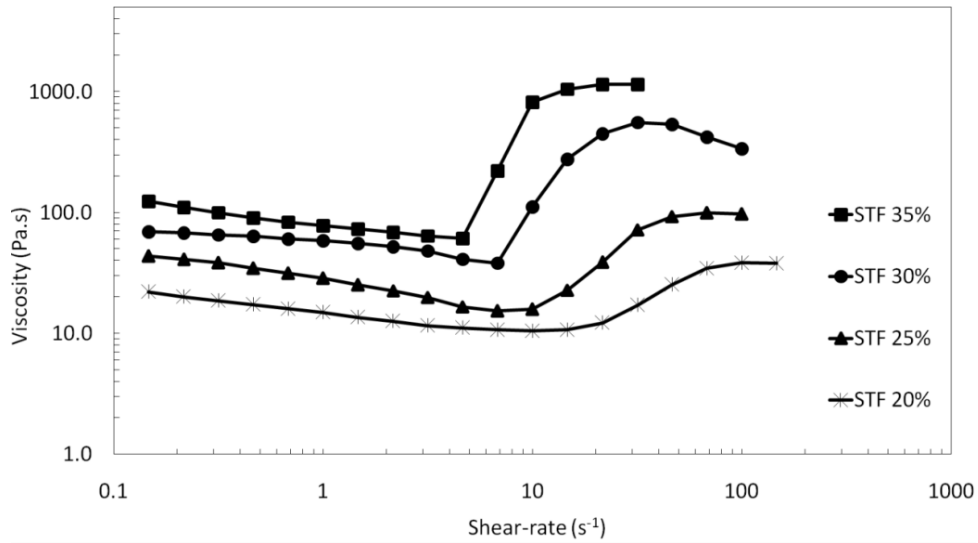


Fig. 2. The shear-rate sweep curves for the 20, 25, 30, and 35 wt% STF.

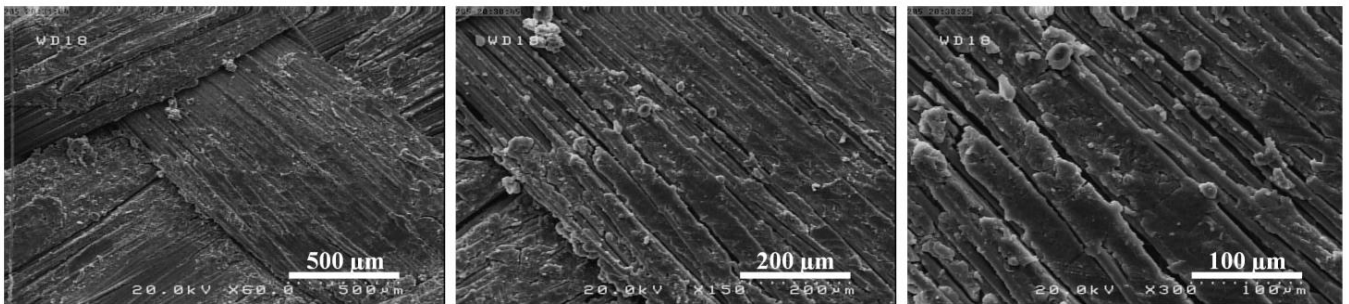


Fig. 3. The FE-SEM images of the impregnated 3D-glass fabrics; (a) $\times 60$ magnification of STF(30) impregnated 3D-glass fabric, (b) $\times 150$ magnification, (c) $\times 300$ magnification.

revealed the STF approximately was well dispersed across the fibers of the 3D-glass fabric, as well as has dispersed uniformly enough over the fabric surface. By the mechanical mixing and sonication method, the homogeneous STF and a uniform impregnated 3D-glass fabric was gained.

2- 6- Quasi-static puncture test

To investigate the quasi-static puncture resistance of the STF impregnated fabrics, the puncture test was performed by using a Universal Testing Machine (STM-250). The test was performed in a similar way as the compressive stress test and loaded by a puncture needle oriented normal to the sample surface. The loading rate was 300 mm/min and the puncture needle has a flat-end cylindrical head in diameter of 7 mm. Fig. 4 is a schematic of the quasi-static puncture test. To hold the samples two circular steel plates of 10 and 20 mm thickness and 200 mm in diameter were selected as fixtures.

The upper part has a square cut out of 10 mm and the bottom part, has a hole in it with a diameter of 40 mm.

The rubber gaskets (5 mm thickness) were used to prevent the slipping of the samples. According to the processing of the data from the load-cell of the UTM, the load vs. displacement curve as the output diagram was obtained and recorded. The samples of higher puncture resistance showed a higher peak force. The quasi-static puncture tests were performed on a single-ply layer of neat and STF impregnated Kevlar, 2D, and 3D-glass fabrics as shown in Fig. 5.

2- 7- Analyses of quasi-static puncture test data

The quasi-static puncture test was carried out on the 20, 25, 30, and 35 wt% STF impregnated 3D-glass fabrics to examine the influence of STF concentration on the performance of the considered samples. It should be noted that the 3D-glass fabric impregnated with the STF of 40 wt%

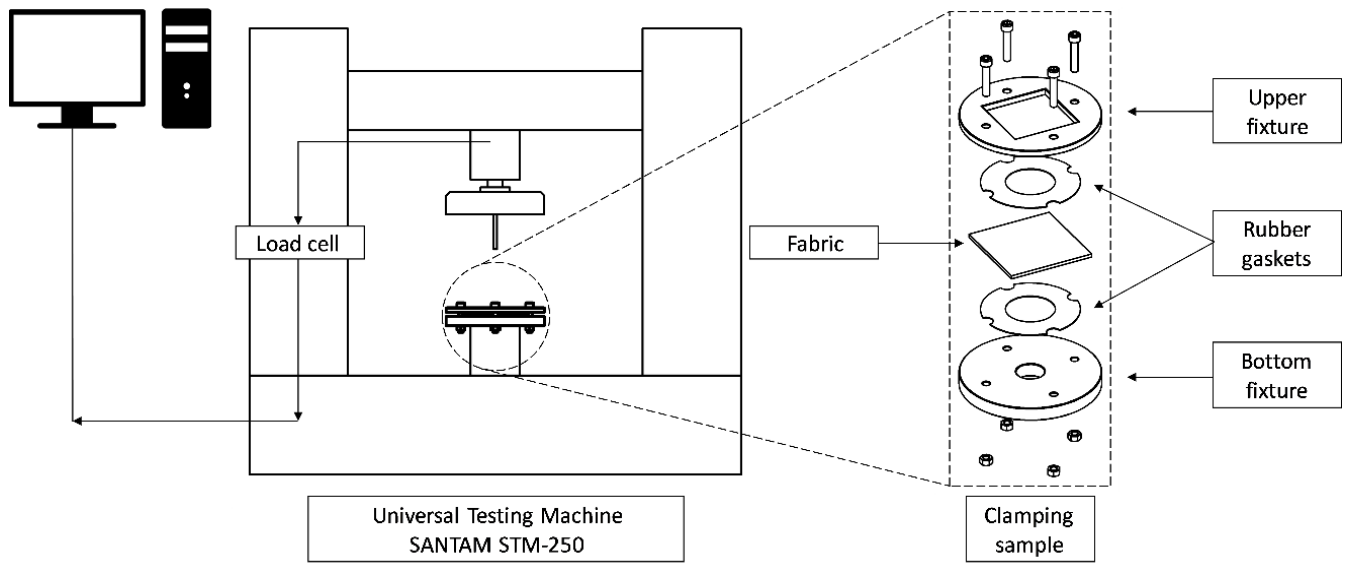


Fig. 4. Schematic of the quasi-static puncture test and sample clamping.

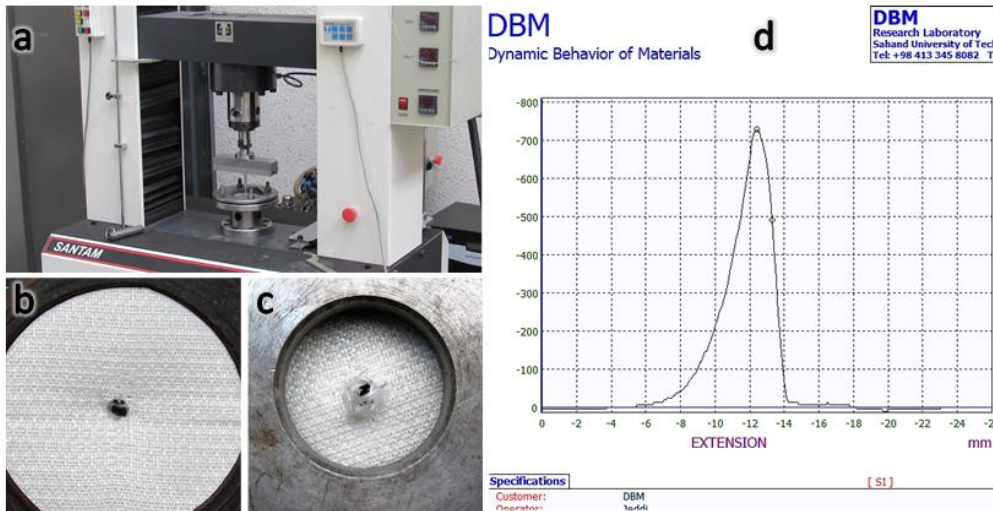


Fig. 5. The quasi-static puncture test: (a) The Universal Testing Machine, (b) front view of sample, (c) rear view of the sample, (d) the load vs. displacement diagram.

silica was prepared. However, the STF did not get wet well, and after the evaporation of the ethanol, most of the silica nanoparticles were poured out like a powder, so no test was performed for this sample. For each case, three puncture tests were performed and according to the results of the tests, the average peak force was obtained. The related load vs. displacement diagrams for the STF (30%) impregnated 3D-glass fabric, are shown in Fig. 6. In order

to compare the performance of the 3D-glass fabric with a high-modulus fiber, the quasi-static puncture test was carried out on a single-ply Kevlar fabric. To investigate the effect of fabric 3D structure and presence of hollow space along the sample's thickness on its performance, the test was also performed on the four-ply 2D-glass fabric (with an areal density of almost equal to a single-ply 3D-glass fabric).

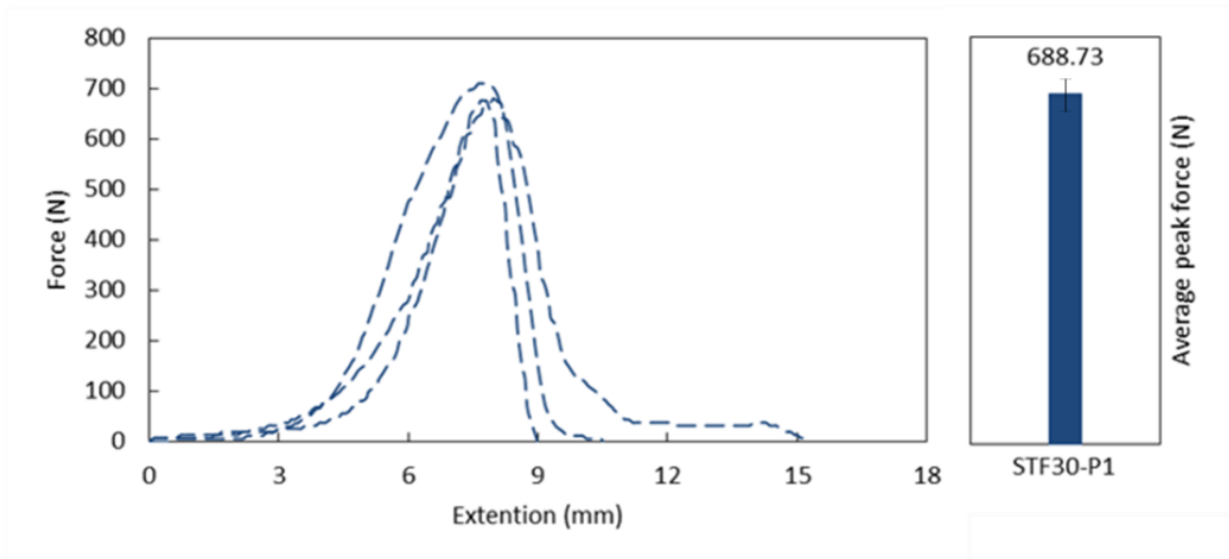


Fig. 6. The load vs. displacement diagram of STF (30% silica) impregnated 3D-glass fabric.

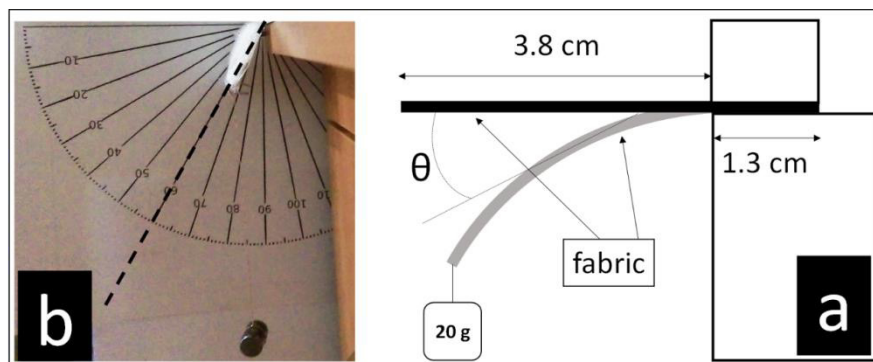


Fig. 7. Schematic of the flexibility test.

2- 8- Flexibility and thickness test

Two-dimensional drape tests (to measure the flexibility) and thickness measurements were performed for the 2D and 3D-glass fabrics in both neat and STF impregnated forms. According to previous methods employed to measure the flexibility [13, 14], the neat and impregnated samples were cut in square format (51×51 mm). Four layers of the 2D-glass and one layer of the 3D-glass fabric were prepared in both neat and STF impregnated form. In all cases, a 20 g weight was attached to the samples as shown in Fig. 7. The bending angle (θ) as a measure of sample flexibility was recorded. A digital caliper and a micrometer were used to measure the sample's thickness.

3- Results and Discussion

3- 1- Add-on % results

As previously mentioned, the weight of samples was determined before and after the STF impregnation process. The average weight of the neat and impregnated fabrics with various STFs and the weight add-on % results are presented in Table 3.

3- 2- Quasi-static puncture results

The quasi-static puncture test was performed by using the STM-250 (UTM). Figs. 8 and 9 show the damage of samples after the quasi-static puncture tests.

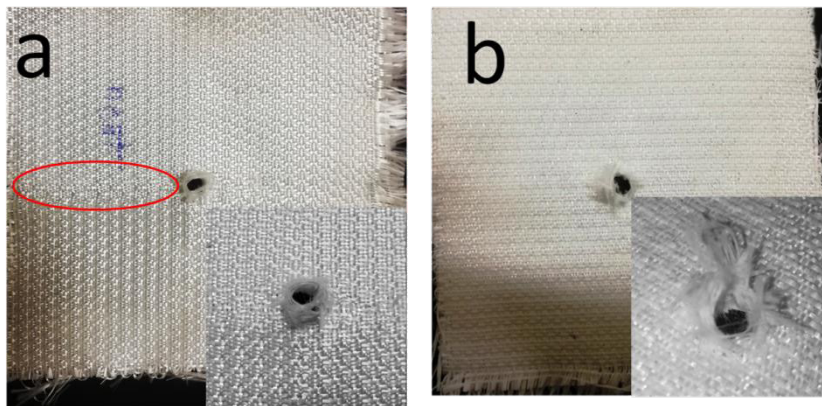


Fig. 8. The photographs of 3D-glass samples damage after the quasi-static puncture tests; (a) neat 3D-glass fabric, (b) 30 wt% STF impregnated 3D-glass fabric.

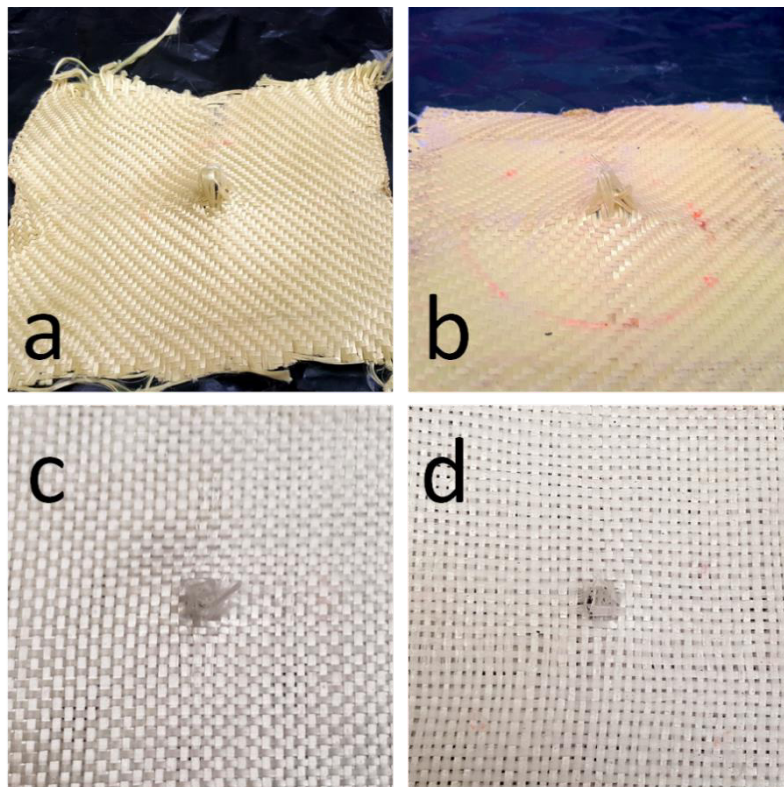
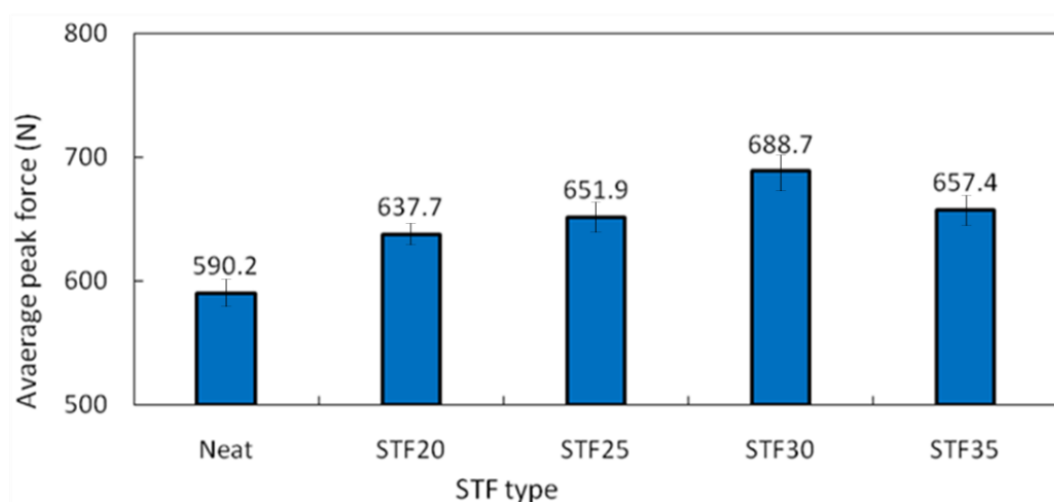


Fig. 9. The photographs of the damage attributed to the single-ply Kevlar and four-ply 2D-glass fabric after the quasi-static puncture tests; (a) neat single-ply Kevlar fabric, (b) 30 wt% STF impregnated single-ply Kevlar fabric, (c) neat four-ply 2D-glass fabric, (d) 30 wt% STF impregnated four-ply 2D-glass fabric.

Table 3. Add-on % results based on the concentration variation of the STF

Sample	Neat Areal Density (g/m ²)	Impregnated Areal Density (g/m ²)	Add-on (%)
3D-glass Neat	837	-	-
2D-glass Neat	201	-	-
3D-glass-20	859	1099	28
3D-glass-25	842	1061	26
3D-glass-30	857	1057	23
Kevlar-30	407	445	9
2D-glass-30	201	234	17
3D-glass-35	841	1013	20

**Fig. 10. Comparison of the puncture resistance (average peak force) of neat and various STFs (20% silica, 25% silica, 30% silica, and 35% silica) impregnated 3D-glass fabrics.**

It can be seen that the puncture damage in the neat fabrics, mainly caused by the yarn pull-out with little fiber tearing or fracture of fibers. It indicates, fewer fibers are involved and resist against the quasi-static puncture. However, in the impregnated samples it was revealed the damage caused chiefly by the fibers tearing, and the yarn pull-out was less observed. It should be noted the difference in damage form in the neat and STF impregnated 3D-glass fabrics was more tangible. From Fig. 10, it can be concluded the puncture resistance of the STF impregnated 3D-glass fabrics relative to the neat fabric increases by raising the silica concentration in the STF from 20 to 30 wt%. However, the performance of the 35 wt% STF impregnated sample was reduced.

There is not sufficient friction among the fibers of the neat fabric, and the fibers can be slid. Therefore, the puncturing needle can pass through the fibers easily and push aside them. In the case of the STF impregnated fabrics, the STF existing among the fibers prevents the fibers from sliding. It indicates when the quasi-static loading is applied on the STF impregnated fabrics; the STF plays a significant role in increasing the interface friction among their yarns and fibers. According to the yarn pull-out test results, the STF impregnation increases the yarn pull-out force by filling in the hollow spaces inside the fabrics and among the gaps where the fibers cross. Considering the low-rate of the loading, the main reason for the improvement of the puncture resistance

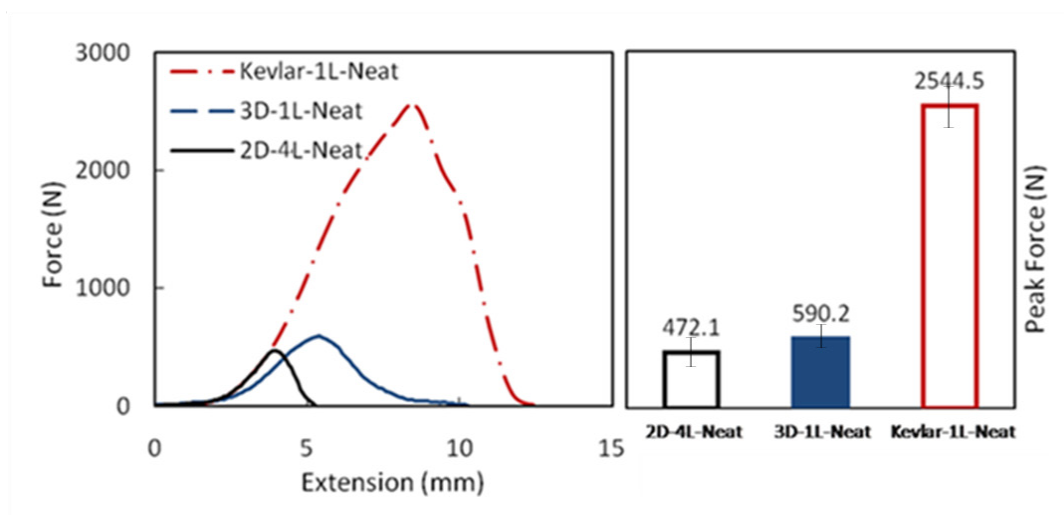


Fig. 11. Comparison of the load vs. displacement diagram of neat single-ply 3D-glass fabric and Kevlar, also four-ply 2D-glass fabric.

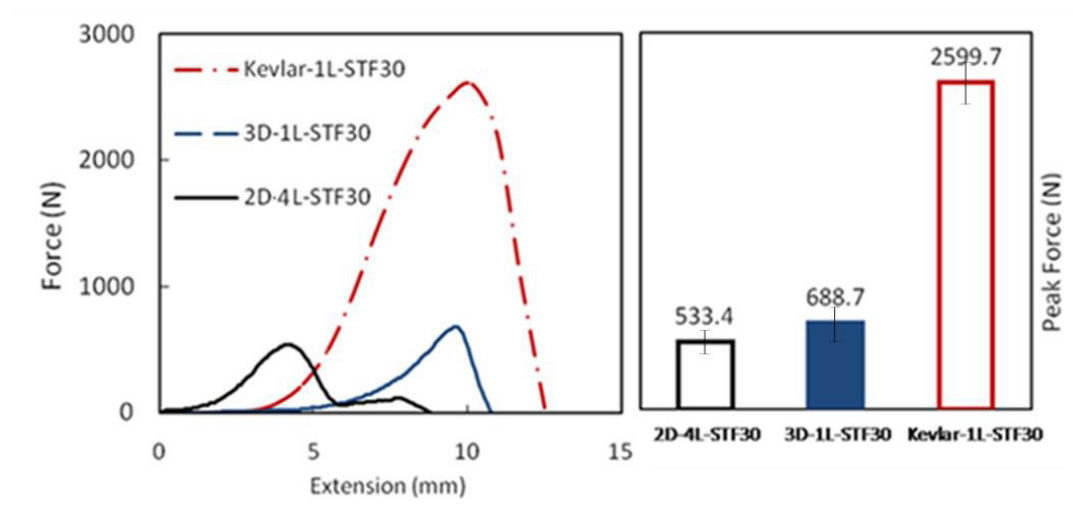


Fig. 12. Comparison of the load vs. displacement diagram of STF (30% silica) impregnated single-ply 3D-glass fabric and Kevlar, also four-ply 2D-glass fabric.

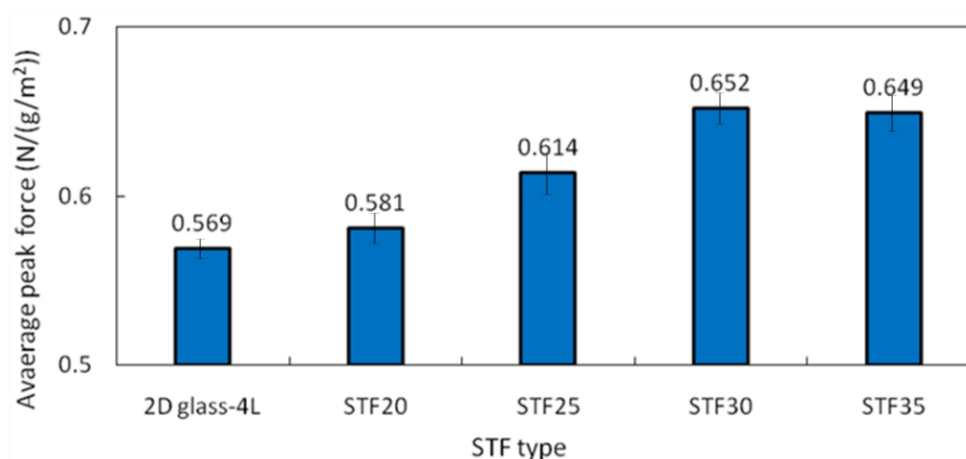
of the impregnated samples with high-concentrated STF is its increased viscosity and consequently increased the interface friction of the fabric among its yarns and fibers rather than the shear-thickening behavior. As shown in Fig. 10, the performance of the 35 wt% STF impregnated sample was reduced, while Table 3 shows a lower weight increase (add-on %) for this sample. This could be due to the excessive concentration of the silica nanoparticles in the STF and consequently, the loss of fluidity of the STF. This makes the fabric not wet well and the friction among the fibers to be reduced again. Figs. 11 and Fig. 12 show

the quasi-static puncture test results and comparison of the load vs. displacement diagrams of the neat and 30 wt% STF impregnated single-ply Kevlar, 3D-glass, and four-ply 2D-glass fabrics.

As predicted, the results revealed the 2D and 3D-glass fabrics have a considerably lower puncture resistance than the Kevlar fabric. It can be due to the high modulus of the Kevlar. It should be noted the structure of the fabric's surface has a significant role in puncture resistance. However, in this study, just the areal density of the 3D and 2D-glass fabrics was considered. From the figures it is apparent the STF

Table 4. The results for the quasi-static puncture resistance tests

Test Case	Puncture Resistance Peak Force (N)	Increased Resistance Force (%)
3D-glass Neat	590	-
2D-glass-4L Neat	472	-
Kevlar Neat	2544	-
3D-glass-20	637	8.1
3D-glass-25	651	10.4
3D-glass-30	688	16.7
3D-glass-35	657	11.4
Kevlar-30	2599	2.2
2D-glass-4L-30	533	12.9

**Fig. 13. Comparison of the samples peak force in same areal density**

impregnated 3D-glass fabric has a higher puncture resistance than the four-ply 2D-glass fabric. It can be related to the 3D structure of the sample. It indicates the hollow spaces inside the 3D-glass fabric, leading to the remaining more quantity of the STF. According to the results of the yarn pull-out test, the STF impregnation and its remaining inside the fabric or among the fibers leads to an increase in the yarn pull-out force and consequently the puncture resistance of the sample.

The results show that, among all the impregnated 3D-glass fabrics, the 30 wt% STF impregnated 3D-glass fabric gave better performance and displayed the most puncture resistance. The amount of peak force endured by this type of impregnated 3D-glass fabric was 16.7% higher than the neat 3D-glass fabric. Due to the low-velocity of the loading, the main role of the

STF in increasing the puncture resistance of the impregnated fabrics as the rheological test showed, is the viscosity of the STF and increase in friction among the fibers of the sample. As previous studies have shown; by increasing the concentration of the silica nanoparticles, the shear-thickening effect and the viscosity of the STF increase. Increasing the viscosity leads to increased friction, and this causes more fibers to resist the quasi-static puncture. Table 4 shows the average peak force for each sample and a comparison among them.

Fig. 13 shows the puncture test results of the neat and the STF impregnated samples in the same areal density.

The results revealed in the same areal density; the best sample (30 wt% silica nanoparticle) has the best performance and four-ply 2D-glass fabrics have much lower performance.

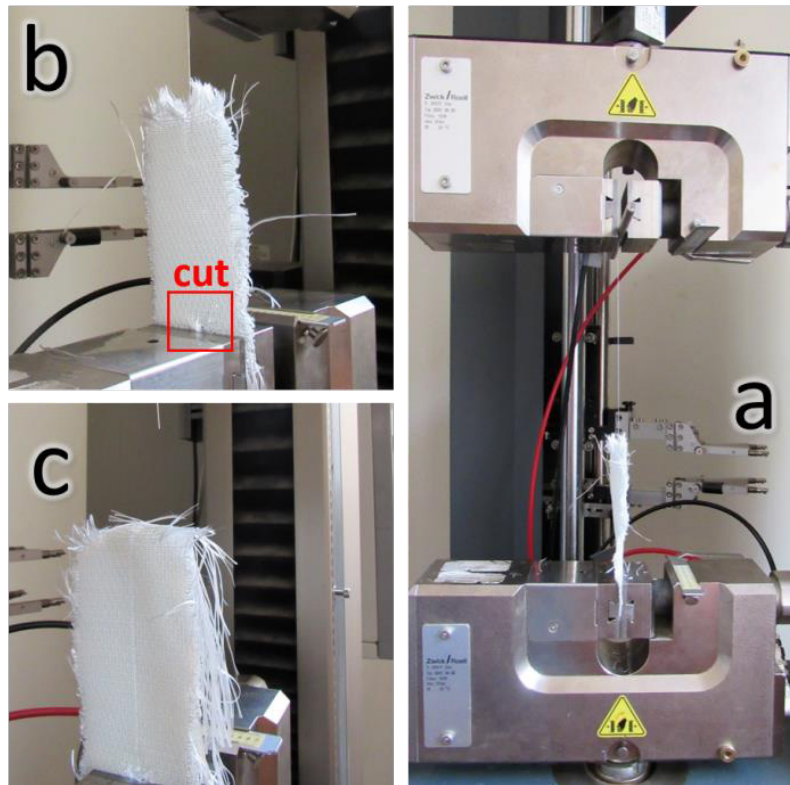


Fig. 14. The yarn pull-out test; (a) the Zwick Roell Z010 (UTM), (b) the created cut, (c) pulled-out yarn.

3- 3- Yarn pull-out test

Due to the 3D and braided structure of the 3D-glass fabrics, and the notable difference with the weave pattern of the 2D-glass and Kevlar (plain and twill weave), the comparison of their yarn pull-out performance will be inaccurate. Because the weave pattern of a sample will undoubtedly affect the force required to pull out its yarn. Therefore, the single warp yarn pull-out test was carried out using a universal testing machine (Zwick Roell Z010) just to investigate the effect of the STF impregnation process on the inter-yarn mobility and interface friction among the yarns of the 3D-glass fabric. Accordingly, the sample was cut in 65×127 mm, and then the middle single warp yarn of the neat and 30 wt% STF impregnated fabric, were pulled out at a loading rate of 200 mm/min. Fig. 14 shows the yarn pull-out test, in which the sample is clamped along its edges, and to prevent elastic deformation of the fabric's yarn as it can be seen in the figure, a cut has been created below the single yarn.

Fig. 15 demonstrates the yarn pull-out test results and load-displacement diagrams for the neat and 30 wt% STF impregnated 3D-glass fabrics.

As it can be seen, the peak yarn pull-out force of the neat and 30 wt% STF impregnated fabrics have been obtained 2.5

and 6 N respectively. It indicates the STF impregnation has caused to engage more and more fibers and has restricted the movement of the yarn during the yarn pull-out, which provides a considerable effect in increasing the peak load at the yarn pull-out test.

3- 4- Flexibility and thickness test results

The flexibility tests revealed the impregnation of the 2D-glass fabrics with the STF has little effect on their flexibility. As shown in Table 5, the bending angle of the neat and impregnated fabrics in this type of samples is approximately equal. However, for the STF impregnated 3D-glass fabrics, the bending angle has changed and their flexibility has slightly decreased, which can be attributed to their 3D dimensional structure and consequently, more STF remaining in these fabrics.

From Table 5, it can be concluded the thickness of the STF impregnated 2D-glass fabric is further increased, which can be attributed to the 2D structure of the sample, and the STF remaining on the fabric surface after the impregnation process. However, for the 3D-glass fabric, most of the STF remains in the hollow space inside the sample.

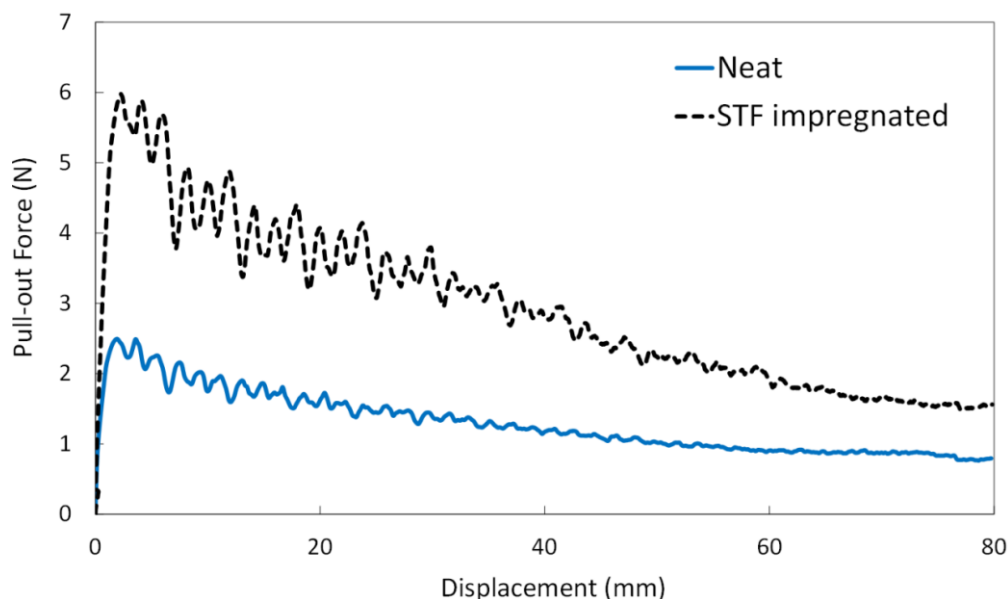


Fig. 15. The yarn pull-out diagrams of the neat and 30 wt% STF impregnated 3D-glass fabrics.

Table 5. The flexibility and thickness test results

Test Case	Bending Angle (θ)	Thickness (mm)
3D-glass Neat	60°	50.00
2D-glass-4L Neat	75°	00.73
3D-glass-30	50°	50.18
2D-glass-4L-30	75°	00.93

4- Conclusions

The development of low cost, lightweight, and wearable protection clothing is the main objective of body armor research. Considering the high price of Kevlar fabrics and the ever-increasing use of glass fabrics as reinforcement in various composites, in this study, the quasi-static puncture resistance of neat (non-impregnated) and Shear Thickening Fluid (STF) impregnated 3D-glass fabrics was investigated at different concentrations of STF. The results were compared with Kevlar and four-ply 2D-glass fabrics. The STF mixture was prepared by dispersing silica nanoparticles (12 nm) in the Polyethylene Glycol (PEG) with a molecular weight of 400 g/mol using the combination of mechanical mixing and the sonication method. The puncture resistance of the STF impregnated 3D-glass fabric increases by raising the silica concentration in the STF from 20 to 30 wt%. However, the performance of the 35 wt% STF impregnated sample was reduced. The 2D and 3D-glass fabrics demonstrated a considerably lower puncture resistance than the Kevlar

fabric. Furthermore, the STF demonstrated a lesser impact in increasing the puncture resistance of the Kevlar and the 2D-glass fabric, while the STF effect was more visible to the 3D-glass fabric. The impregnation of 2D-glass fabric with the STF had little effect on its flexibility. However, for the STF impregnated 3D-glass fabric, the bending angle had changed and its flexibility had slightly decreased. The thickness of the STF impregnated 2D-glass fabric is further increased because of the STF persisting on the fabric surface after the impregnation process. However, for the 3D-glass fabric most of the STF remains in the hollow space inside the sample. The main factor of the STF impregnation in improving the performance of samples under the quasi-static puncture and yarn pull-out tests is its increased viscosity and consequently increased the interface friction of the samples among their yarns and fibers. Among all the 3D-glass fabrics, the sample impregnated with the STF of 30 wt% silica nanoparticles, demonstrated the best performance and its puncture resistance was 17% higher than compared to the neat 3D-glass fabrics.

References

- [1] Y. Xu, X. Chen, Y. Wang, Z. Yuan, Stabbing resistance of body armour panels impregnated with shear thickening fluid, *Composite Structures*, 163 (2017) 465-473.
- [2] S. Gürgen, An investigation on composite laminates including shear thickening fluid under stab condition, *Journal of Composite Materials*, 53(8) (2019) 1111-1122.
- [3] C.T. Nguyen, P.I. Dolez, T. Vu-Khanh, C. Gauvin, J. Lara, Effect of protective glove use conditions on their resistance to needle puncture, *Plastics, rubber and composites*, 42(5) (2013) 187-193.
- [4] Q.S. Wang, R.J. Sun, X. Tian, M. Yao, Y. Feng, Quasi-static puncture resistance behaviors of high-strength polyester fabric for soft body armor, *Results in physics*, 6 (2016) 554-560.
- [5] A. Gaurav, K.K. Singh, Safe design fatigue life of CNT loaded woven GFRP laminates under fully reversible axial fatigue: application of two-parameters Weibull distribution, *Plastics, Rubber and Composites*, 48(7) (2019) 293-306.
- [6] R. Umer, H. Alhussein, J. Zhou, W.J. Cantwell, The mechanical properties of 3D woven composites, *Journal of Composite Materials*, 51(12) (2017) 1703-16.
- [7] M. Jeddi, M. Yazdani, Dynamic compressive response of 3D GFRP composites with shear thickening fluid (STF) matrix as cushioning materials, *Journal of Composite Materials*, (2021) 0021998320984247.
- [8] W. Ji, A.M. Waas, Modeling compressive response of 3D woven textile composites accounting for micro scale geometric uncertainties, *Advanced Composite Materials*, 25(2) (2019) 203-223.
- [9] Q. Li, H. Wang, P. Yin, L. Sun, C. Wu, The mechanical properties of damping rubber reinforced by Wrap Knitted Spacer Fabric, *Polymer Composites*, 39(12) (2018) 4434-4441.
- [10] R. Amooyi Dizaji, M. Yazdani, E. Aligholizadeh, A. Rashed, Effect of 3D-woven glass fabric and nanoparticles incorporation on impact energy absorption of GLARE composites, *Polymer Composites*, 39(10) (2018) 3528-3536.
- [11] T.T. Li, L. Ling, X. Wang, Q. Jiang, B. Liu, J.H. Lin, C.W. Lou, Mechanical, acoustic, and thermal performances of shear thickening fluid-filled rigid polyurethane foam composites: Effects of content of shear thickening fluid and particle size of silica, *Journal of Applied Polymer Science*, 136(18) (2019) 47359.
- [12] X. Gong, Y. Xu, W. Zhu, S. Xuan, W. Jiang, W. Jiang, Study of the knife stab and puncture-resistant performance for shear thickening fluid enhanced fabric, *Journal of Composite Materials*, 48(6) (2014) 641-657.
- [13] H.A. Barnes, Shear thickening ("Dilatancy") in suspensions of nonaggregating solid particles dispersed in Newtonian liquids, *Journal of Rheology*, 33(2) (1989) 329-366.
- [14] H. Hasan-nezhad, M. Yazdani, M. Salami-Kalajahi, M. Jeddi, Mechanical behavior of 3D GFRP composite with pure and treated shear thickening fluid matrix subject to quasi-static puncture and shear impact loading, *Journal of Composite Materials*, 54(26) (2020) 3933-3948.
- [15] Y. Park, Y. Kim, A.H. Baluch, C.G. Kim, Empirical study of the high velocity impact energy absorption characteristics of shear thickening fluid (STF) impregnated Kevlar fabric, *International Journal of Impact Engineering*, 72 (2014) 67-74.
- [16] M.J. Decker, C.J. Halbach, C.H. Nam, N.J. Wagner, E.D. Wetzel, Stab resistance of shear thickening fluid (STF)-treated fabrics, *Composites science and technology*, 67(3-4) (2007) 565-578.
- [17] Y.S. Lee, E.D. Wetzel, N.J. Wagner, The ballistic impact characteristics of Kevlar® woven fabrics impregnated with a colloidal shear thickening fluid, *Journal of materials science*, 38(13) (2003) 2825-2833.
- [18] A. Khodadadi, G.H. Liaghat, A.R. Sabet, H. Hadavinia, A. Aboutorabi, O. Razmkhah, M. Akbari, M. Tahmasebi, Experimental and numerical analysis of penetration into Kevlar fabric impregnated with shear thickening fluid, *Journal of Thermoplastic Composite Materials*, 31(3) (2018) 392-407.
- [19] M. Jeddi, M. Yazdani, H. Hasan-nezhad, Energy absorption characteristics of aluminum sandwich panels with Shear Thickening Fluid (STF) filled 3D fabric cores under dynamic loading conditions, *Thin-Walled Structures*, 168 (2021) 108254.
- [20] A. Abbaszadeh, M. Yazdani, F. Abbasi, A. Rashed, Investigating the behavior of silicon-coated Kevlar fabric under low-velocity impact: An experimental and numerical study, *Journal of Thermoplastic Composite Materials*, 32(5) (2019) 635-656.
- [21] R. Wei, B. Dong, F. Wang, J. Yang, Y. Jiang, W. Zhai, H. Li, Effects of silica morphology on the shear thickening behavior of shear thickening fluids and stabbing resistance of fabric composites, *Journal of Applied Polymer Science*, (2019) 48809.
- [22] T.A. Hassan, V.K. Rangari, S. Jeelani, Synthesis, processing and characterization of shear thickening fluid (STF) impregnated fabric composites, *Materials Science and Engineering: A*, 527(12) (2010) 2892-2899.
- [23] R.L. Hoffman, Explanations for the cause of shear thickening in concentrated colloidal suspensions, *Journal of Rheology*, 42(1) (1998) 111-123.
- [24] J. Bender, N.J. Wagner, Reversible shear thickening in monodisperse and bidisperse colloidal dispersions, *Journal of Rheology*, 40(5) (1996) 899-916.
- [25] S. Gürgen, M.C. Kuşhan, W. Li, Shear thickening fluids in protective applications: a review, *Progress in Polymer Science*, 75 (2017) 48-72.
- [26] J.R. Melrose, R.C. Ball, Continuous shear thickening transitions in model concentrated colloids-The role of interparticle forces, *Journal of Rheology*, 48(5) (2004) 937-960.
- [27] Y.S. Lee, E.D. Wetzel, N.J. Wagner, The ballistic impact characteristics of Kevlar® woven fabrics impregnated with a colloidal shear thickening fluid, *Journal of materials science*, 38(13) (2003) 2825-2833.
- [28] T.J. Kang, K.H. Hong, M.R. Yoo, Preparation and properties of fumed silica/Kevlar composite fabrics for application of stab resistant material, *Fibers and Polymers*, 11(5) (2010) 719-724.

List of Figures

Figure. 1. Steps of STF preparation and fabric impregnation: (a) mechanical blending to homogenization, (b) ultrasonication, (c) the container with an inclined plane, (d) the oven to evaporate the ethanol, (e) 3D E-glass fabric PARAGLASS (type-5).

Figure. 2. The shear-rate sweep curves for the 20, 25,30 and 35 wt% STF.

Figure. 3. The FE-SEM images of the impregnated 3D-glass fabrics; (a) $\times 60$ magnification of STF(30) impregnated 3D-glass fabric, (b) $\times 150$ magnification, (c) $\times 300$ magnification.

Figure. 4. Schematic of the quasi-static puncture test and sample clamping.

Figure. 5. The quasi-static puncture test: (a) The Universal Testing Machine, (b) front view of sample, (c) rear view of sample, (d) the load vs. displacement diagram.

Figure. 6. The load vs. displacement diagram of STF (30% silica) impregnated 3D-glass fabric.

Figure. 7. Schematic of the flexibility test.

Figure. 8. The photographs of 3D-glass samples damage after the quasi-static puncture tests; (a) neat 3D-glass fabric, (b) 30 wt% STF impregnated 3D-glass fabric.

Figure. 9. The photographs of damage attributed to the single-ply Kevlar and four-ply 2D-glass fabric after the quasi-static puncture tests; (a) neat single-ply Kevlar fabric, (b) 30 wt% STF impregnated single-ply Kevlar fabric, (c) neat four-

ply 2D-glass fabric, (d) 30 wt% STF impregnated four-ply 2D-glass fabric.

Figure. 10. Comparison of the puncture resistance (average peak force) of neat and various STFs (20% silica, 25% silica, 30% silica and 35% silica) impregnated 3D-glass fabrics.

Figure. 11. Comparison of the load vs. displacement diagram of neat single-ply 3D-glass fabric and Kevlar, also four-ply 2D-glass fabric.

Figure. 12. Comparison of the load vs. displacement diagram of STF (30% silica) impregnated single-ply 3D-glass fabric and Kevlar, also four-ply 2D-glass fabric).

Figure. 13. Comparison of the samples peak force in same areal density

Figure. 14. The yarn pull-out test; (a) the Zwick Roell Z010 (UTM), (b) the created cut, (c) the pulled-out yarn.

Figure. 15. The yarn pull-out diagrams of the neat and 30 wt% STF impregnated 3D-glass fabrics.

List of Tables

Table 1: Specification of the fabrics used in this study

Table 2: The STFs investigated in the present work

Table 3: Add-on % results based on the concentration variation of the STF

Table 4: The results for the quasi-static puncture resistance tests

Table 5: The flexibility and thickness test results

HOW TO CITE THIS ARTICLE

M. Jeddi, M. Yazdani, H. Hasan-nezhad, *Experimental Study on Puncture Resistance of 2D and 3D Glass Fabrics Reinforced with Shear Thickening Fluid*, AUT J. Mech Eng., 6(1) (2022) 31-44.

DOI: [10.22060/ajme.2021.19920.5973](https://doi.org/10.22060/ajme.2021.19920.5973)

